Chapter 2

Elements of theory

In this chapter, the theoretical framework describing the processes we are studying will be summarised. In the first section, the radiative-capture model will be explained. The second section describes the excitation process of a projectile in a target Coulomb field. First, the semiclassical Coulomb-dissociation theory is detailed to justify the use of the virtual-photon method. It is shown how to extract the photonuclear cross section from the Coulomb-excitation cross section and subsequently the radiative-capture cross section. Second, a pure quantum-mechanical model is discussed, which takes account of the nuclear and Coulomb interactions as well as the resulting interferences in the angular distribution of the excited oxygen nucleus. It will be shown that the interference pattern between nuclear and Coulomb processes can be used to measure the pure Coulomb contribution. In a second phase, we will show the sensitivity of the fragment angular correlation to the multipolarity of the excitation process and thus the necessity of the correlation measurement to separate the various multipole contributions.

2.1 Radiative capture

2.1.1 Coulomb-barrier penetration

The relative energy is referred to as the sum of the centre-of-mass kinetic energies of two colliding particles, given in the non-relativistic case by $\varepsilon = \mu v^2/2$, where μ is the reduced mass and v is the rela-

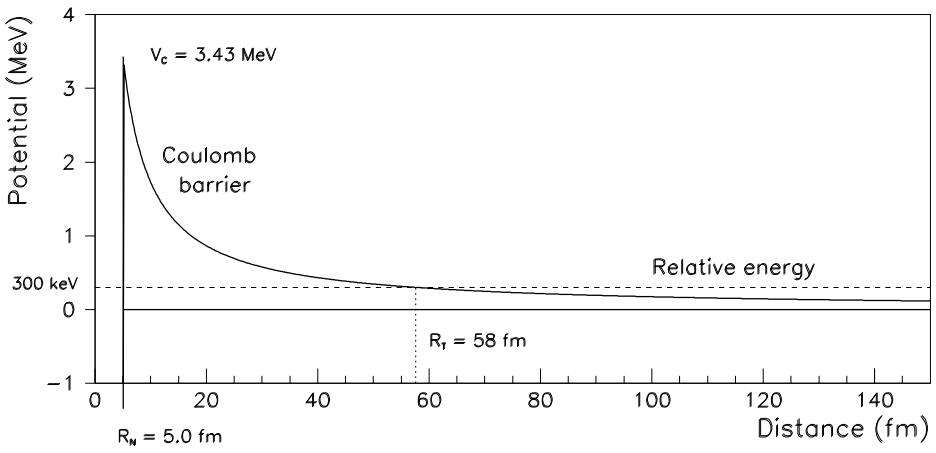

Figure 2.1: *The Coulomb barrier classically prevents low-energy particles to approach each other. The nuclear potential is here described as a square well. The relative energy of about 300 keV corresponds to the Gamow-peak energy (see also fig. 2.2).*

tive velocity, i.e. the sum of the velocities in the centre of mass. The distribution of the relative energy in a stellar medium is described by the Maxwell-Boltzmann distribution, and thus the mean relative-energy value is $3kT/2$, i.e. 26 keV at 2×10^8 K. The Coulomb barrier of the ^{12}C+α system is approximately $V_C = Z_C Z_\alpha e^2/R_N \simeq 3.43$ MeV (see fig. 2.1), where $R_N \simeq 5.0$ fm is the the sum of the nuclear radii. Therefore, the Coulomb barrier between ^{12}C and α is far higher than the average thermal energy. Particles in a 26-keV thermalised system would not approach one another closer than $R_T = 665$ fm (the classical turning point). The normalised abundance of particles above V_C at this temperature is calculated by integration of the Maxwell-Boltzmann distribution from V_C up to infinity, which gives approximately 10^{-85}. Therefore, it is classically excluded to cross the barrier and it is essential to consider the quantum-mechanical tunnelling.

The probability to find a particle at a position r is given by $|\psi(r)|^2$. Therefore, the probability that an incoming particle be found inside the

nucleus at R_N relative to finding it at the turning point R_T is given by

$$T = \frac{|\psi(R_N)|^2}{|\psi(R_T)|^2}\,. \tag{2.1}$$

The solution of the Schrödinger equation for a particle of energy ε in a broad and high potential $V(r)$, calculated by the Wentzel-Kramers-Brillouin (WKB) approximation [Mer61], gives a penetration factor of [Bet47]

$$T \simeq \exp\left(-\frac{2}{\hbar}\int_{R_T}^{R_N}\sqrt{2\mu(V(r)-\varepsilon)}\,dr\right)\,, \tag{2.2}$$

where μ is the reduced mass. This is equal to [Rol88]

$$T \simeq \exp\left[-2KR_T\left(\frac{\arctan\sqrt{R_T/R_N-1}}{\sqrt{R_T/R_N-1}}-\frac{R_N}{R_T}\right)\right]\,, \tag{2.3}$$

where $K=\sqrt{2\mu(V_C-\varepsilon)}/\hbar$.

The multiplication of the penetration factor with the Maxwell-Boltzmann distribution shows a maximum at approximately 300 keV called the Gamow peak, with a FWHM of about 170 keV (fig. 2.2). By integrating the Gamow peak over the energy, the fraction of particle pairs passing through their Coulomb barrier at 2×10^8 K is found to be about 10^{-16}, which is sufficient to induce the reaction in the star [Rol88]. This abundance is extremely sensitive to the temperature, for instance, reducing the temperature by a factor of two would decrease the reaction yield by a factor of one million.

2.1.2 The S factor

The radiative-capture cross section σ^{cap} of ^{12}C and α is proportional to the interacting area of the involved nuclei, given quantum-mechanically by $\pi\lambda\!\!\!^{-2}$, where $\lambda\!\!\!^{-}=\hbar/\sqrt{2\mu\varepsilon}$ is the reduced wavelength of the system. This is multiplied with the transition probability $T_{\Pi l}$ of the given channel l (Π symbolising E or M, i.e. electric or magnetic multipolarity) and with the number of corresponding available substates. Thus, the cross section for spinless, non-identical particles is written

$$\sigma^{cap}_{\Pi l}(\varepsilon) = \frac{\pi\hbar^2}{2\mu\varepsilon}(2l+1)T_{\Pi l}\,. \tag{2.4}$$

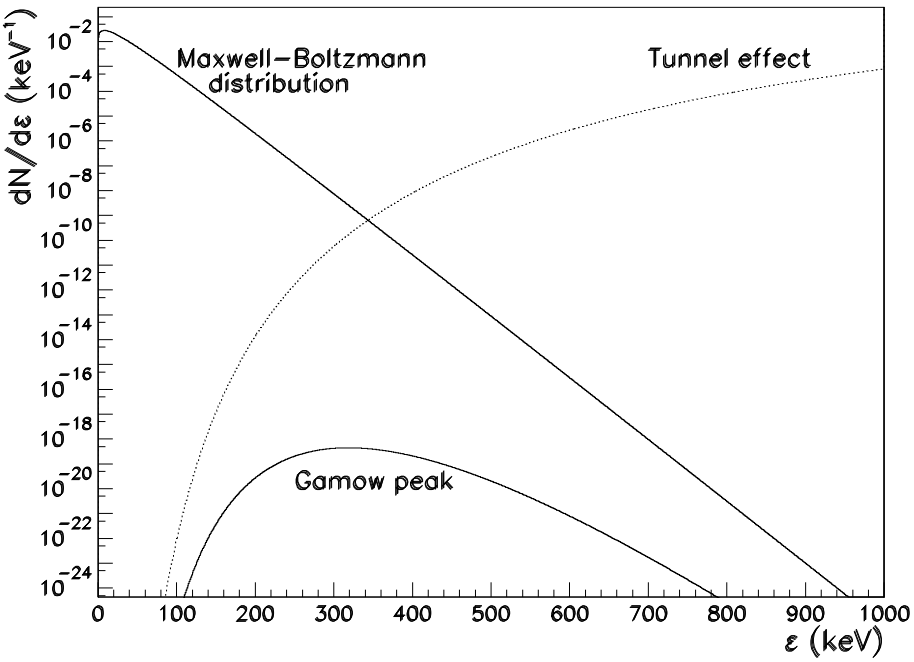

Figure 2.2: *The Gamow peak at approximately 300 keV is the product of the Maxwell-Boltzmann distribution with the tunnelling probability for a radiative-capture reaction* $^{12}C+\alpha$ *in a thermal system at* $T = 2 \times 10^8$ *K. This is the energy region where the reaction is more likely to take place. At higher energies the number of particles becomes insignificant while at lower energies the tunnelling through the Coulomb barrier makes the reaction improbable. The dimension of the Maxwell-Boltzmann distribution and of the Gamow peak is* keV^{-1}*, while the tunnelling probability is dimensionless.*

The total capture cross section for a given transition is thus

$$\sigma^{cap}(\varepsilon) = \sum_l \sigma^{cap}_{El}(\varepsilon) + \sigma^{cap}_{Ml}(\varepsilon)\,. \tag{2.5}$$

Traditionally, the total cross section is written in the form

$$\sigma^{cap}(\varepsilon) = S(\varepsilon)\,\frac{1}{\varepsilon}\,\exp(-2\pi\eta)\,, \tag{2.6}$$

where $1/\varepsilon$ represents the energy dependence of the de Broglie wavelength and $e^{-2\pi\eta}$ is a parameter containing the exponential dependence of the transition probabilities (originally a tunnelling probability approximation valid for light particles, following eq. 2.3), and

$$\eta = \frac{Z_C Z_\alpha e^2}{\hbar}\sqrt{\frac{\mu}{2\varepsilon}} \tag{2.7}$$

is the Sommerfeld (or Coulomb) parameter. $S(\varepsilon)$ is referred to as the 'astrophysical factor' (or sometimes 'nuclear factor'). It is a more convenient, smoothly-varying function containing the nuclear information and the normalisation of the cross section.

2.1.3 Decomposition of the capture probabilities

Once the geometrical cross section has been defined, it is necessary to calculate the matrix elements that determine the reaction probabilities via the radiative-capture model, which is presented here following Blatt and Weisskopf [Bla79].

In this approach, the fusion of ^{12}C and α can be seen as a radiative transition of a system from an unbound state $|\psi_{C\alpha}\rangle$ to a bound state $|\psi_{O^*}\rangle$. This system is characterised by charge and current densities, the matrix elements of which are given by, respectively,

$$\rho(\vec{r}) = e\,\psi^*_{C\alpha}(\vec{r})\,\psi_{O^*}(\vec{r})\,, \tag{2.8}$$

$$\vec{\jmath}(\vec{r}) = \frac{e}{2\mu}\left[\psi^*_{C\alpha}\,(\vec{\mathcal{P}}\,\psi_{O^*}) + (\vec{\mathcal{P}}\,\psi_{C\alpha})^*\,\psi_{O^*}\right]\,, \tag{2.9}$$

where $\vec{\mathcal{P}} = -i\hbar\vec{\nabla}$ is the momentum operator. These generate the outgoing varying electromagnetic fields $\vec{E}(\vec{r})\,e^{-i\omega t}$ and $\vec{H}(\vec{r})\,e^{-i\omega t}$ for the

energy component $\hbar\omega$. These fields can be expressed in the form of multipole elements in order to integrate over space the time-averaged energy carried away by the wave. The photon emission probability per unit time, i.e. the radiative transition probability per unit time, is then extracted by calculating the ratio of this energy to that of one photon $E_\gamma = \hbar\omega$. The corresponding transition amplitudes (approximated for a wavelength large compared to the dimension of the source) are then given by

$$a^{cap}_{Elm} \simeq \left(\frac{8\pi}{\hbar}\,\frac{l+1}{l}\right)^{\frac{1}{2}} \frac{k_\gamma^{l+\frac{1}{2}}}{(2l+1)!!}\int_\tau \rho(\vec{r}) r^l\, \mathcal{Y}^*_{lm}(\theta,\phi)\, d\tau\,, \tag{2.10}$$

$$a^{cap}_{Mlm} \simeq -\frac{i}{c(l+1)}\left(\frac{8\pi}{\hbar}\,\frac{l+1}{l}\right)^{\frac{1}{2}} \frac{k_\gamma^{l+\frac{1}{2}}}{(2l+1)!!}\times \int_\tau \vec{\jmath}(\vec{r})\cdot\vec{\mathcal{L}}\, r^l\, \mathcal{Y}^*_{lm}(\theta,\phi)\, d\tau, \tag{2.11}$$

where τ is the volume of the system, k_γ is the wave number of the photon, $\mathcal{Y}_{lm}$ is a spherical harmonics and $\vec{\mathcal{L}} = -i\vec{r}\times\vec{\nabla}$ is the angular-momentum operator. The notation 'double factorial' is defined as $(2l+1)!! = 1 \times 3 \times ... \times (2l+1)$.

In the long-wavelength approximation, the matrix elements of the electric and magnetic multipole moments are defined for a given multipolarity, respectively, as [Boh69]

$$\langle\psi_{O^*}|\,\mathcal{M}_{Elm}\,|\psi_{C\alpha}\rangle \simeq \int_\tau \rho(\vec{r})\, r^l\, \mathcal{Y}_{lm}(\theta,\phi)\, d\tau\,, \tag{2.12}$$

$$\langle\psi_{O^*}|\,\mathcal{M}_{Mlm}\,|\psi_{C\alpha}\rangle \simeq -\frac{i}{c(l+1)}\int_\tau \vec{\jmath}(\vec{r})\cdot\vec{\mathcal{L}}\, r^l\, \mathcal{Y}_{lm}(\theta,\phi)\, d\tau. \tag{2.13}$$

They depend on the structure of the system and thus on the collision dynamical parameters. These contain the isoscalar and isovector contributions [Bay83]. In isospin formalism (i.e. writing the nucleon charge $e_k = (1/2 - t_{zk})e$, where t_{zk} is the third component of the isospin vector of the k^{th} nucleon) it is trivial to show that the isoscalar term is zero for a dipole electric transition.

Inserting eqs. 2.8, 2.9, 2.12 and 2.13 into eqs. 2.10 and 2.11, and making use of the property $\mathcal{Y}^*_{lm} = (-1)^m\, \mathcal{Y}_{l\,-m}$, the transition amplitudes

from state $|\psi_{C\alpha}\rangle$ to state $|\psi_{O^*}\rangle$ can be rewritten in the general form

$$a^{cap}_{\Pi lm} = (-1)^m \left(\frac{8\pi}{\hbar}\,\frac{l+1}{l}\right)^{\frac{1}{2}} \frac{k_\gamma^{l+\frac{1}{2}}}{(2l+1)!!} \langle\psi_{O^*}|\,\mathcal{M}_{\Pi l\,-m}\,|\psi_{C\alpha}\rangle\ . \quad (2.14)$$

The radiative capture probability per unit time $P^{cap}_{\Pi lm} = |a^{cap}_{\Pi lm}|^2$ is then given by

$$P^{cap}_{\Pi lm} = \frac{8\pi(l+1)}{l(2l+1)!!^2}\frac{1}{\hbar}\left(\frac{E_\gamma}{\hbar c}\right)^{2l+1} |\langle\psi_{O^*}|\,\mathcal{M}_{\Pi l\,-m}\,|\psi_{C\alpha}\rangle|^2\ . \quad (2.15)$$

The orientation of the substates being not relevant for the transition probabilities, only the average probability over the substates m is considered. The total capture probability is given for spinless particles by $P^{cap}_{\Pi l} = \sum_m P^{cap}_{\Pi lm}$. Note that this is only valid for spinless particles, for a more general reaction a(b,γ)c the probability must be averaged over the initial substates and summed over the final states such that the statistical factor becomes $(2I_c+1)/(2I_a+1)(2I_b+1)$, where I_a, I_b and I_c are the spins of the particles.

The cross section of two colliding nuclei is defined by the ratio of the transition probability per unit time to the incident flux, summed over the final substates and averaged over the initial substates. For spinless particles, and defined for a unit-flux scattering wave function, this is given by [Bay83]

$$\sigma^{cap}_{\Pi l}(\varepsilon) = (2l+1)\frac{8\pi(l+1)}{l(2l+1)!!^2}\frac{1}{\hbar}\left(\frac{E_\gamma}{\hbar c}\right)^{2l+1} B^{cap}_{\Pi l}(\varepsilon)\,, \quad (2.16)$$

where $B^{cap}_{\Pi l}$ is the 'reduced transition probability' between an unbound state and a bound state, containing the nuclear information and the dynamical parameters of the collision. It is strongly model-dependent and defined as

$$B^{cap}_{\Pi l} = \sum_m |\langle\psi_{O^*}|\,\mathcal{M}_{\Pi l\,-m}\,|\psi_{C\alpha}\rangle|^2\ . \quad (2.17)$$

For an isolated narrow resonance (and as an approximation for a broad resonance) the radiative-capture cross section of spinless particles is described by the Breit-Wigner formula [Val89b]:

$$\sigma^{cap}_{\Pi l}(\varepsilon) = \frac{\pi\hbar^2}{2\mu\varepsilon}\,(2l+1)\,\frac{\Gamma_\alpha\Gamma_\gamma}{(\varepsilon-\varepsilon^*)^2+(\Gamma/2)^2}\,, \quad (2.18)$$

where ε^* is the energy of the resonance in the centre of mass, and Γ, Γ_γ and Γ_α are the total, radiative and α widths, respectively. Comparing eq. 2.18 and eq. 2.16, the reduced capture probability is written

$$B^{cap}_{\Pi l}(\varepsilon) = \frac{\pi\hbar^3}{2\mu\varepsilon}\,\frac{l(2l+1)!!^2}{8\pi(l+1)}\,\left(\frac{\hbar c}{E_\gamma}\right)^{2l+1}\frac{\Gamma_\alpha\Gamma_\gamma}{(\varepsilon-\varepsilon^*)^2+(\Gamma/2)^2}\,. \tag{2.19}$$

2.2 Coulomb dissociation

2.2.1 Principle

The Coulomb-dissociation method consists in using the fact that a projectile passing by a target nucleus sees the differential Coulomb field as an electromagnetic pulse (fig. 2.3), which is in QED interpreted as a virtual photon according to the Weizsäcker-Williams virtual-quanta method [Jac75]. The target nucleus is chosen to be ^{208}Pb because of a strong Coulomb field and the relatively low density of the low-lying excited states, i.e. a low probability for target excitation. The pulse time (or collision time) can be approximated by $\tau_c \simeq b/2\gamma V$, where b is the impact parameter, V is the beam velocity and γ is the Lorentz factor. An excitation from the ground state to a state at energy E^* is only possible when the collision time is shorter than the transition time $\tau_t = \hbar/E^*$, otherwise the nucleus reacts adiabatically. This is described by the adiabaticity parameter [Tat96]

$$\xi = \frac{\tau_c}{\tau_t} = \frac{bE^*}{2\gamma V\hbar} \lesssim 1\,. \tag{2.20}$$

Because of the condition of adiabaticity the Coulomb-dissociation process favours low excitation energies, thus low relative energies between fragments after breakup, which makes it useful for astrophysical purposes. The resonant breakup is referred to as a sequential process since the life time of a resonance $\tau = \hbar/\Gamma$ (3×10^5 and 2×10^3 fm/c for the levels at 9.58 and 9.84 MeV in ^{16}O), where Γ is the width, is much larger than the collision time (18 fm/c for $E_{rel} = 80$ MeV/u relative energy between ^{16}O and ^{208}Pb at a 15-fm impact parameter). In case of a direct breakup, the process is assumed to be instantaneous, nevertheless the time needed for the fragments to separate is estimated to be $(R_\alpha + R_C)/v$ [Bau94],

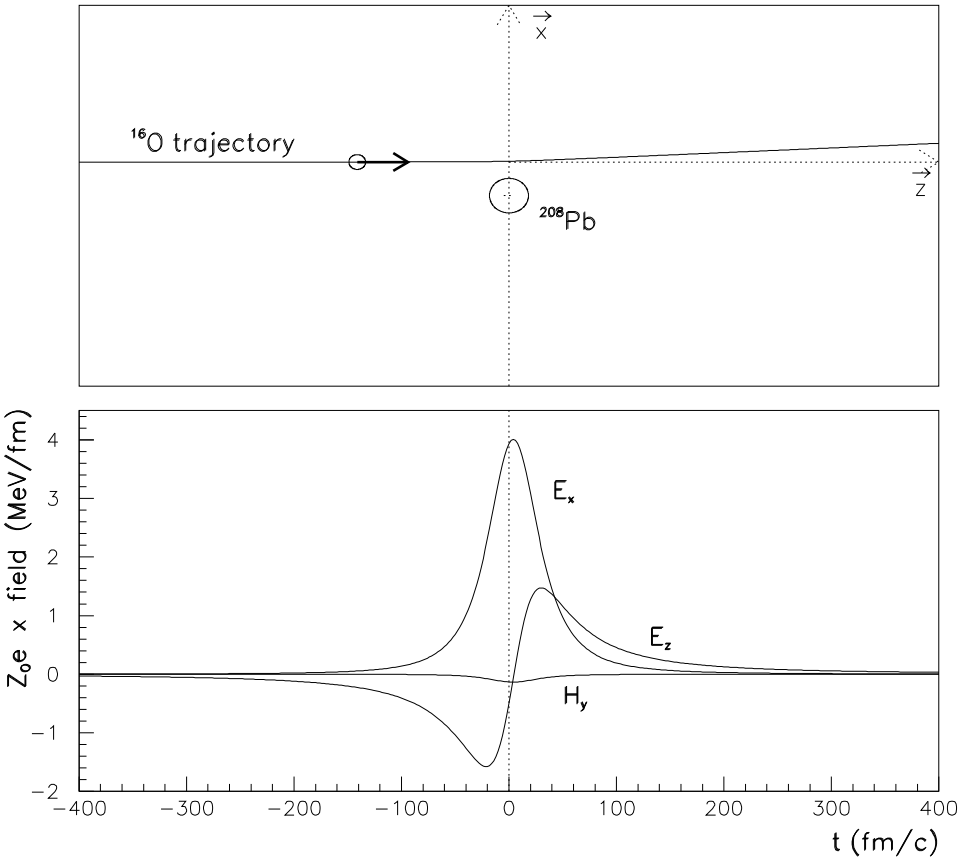

Figure 2.3: *Field components of the electromagnetic pulse in the ^{16}O projectile passing by a ^{208}Pb nucleus, for an energy of 80 MeV/u and an impact parameter of 15 fm.*

where R_C and R_α are the ^{12}C and α radii, respectively, and v is the fragments' relative velocity. This time is still relatively long for low energies (115 to 340 fm/c for 2.7 MeV to 300 keV) and the direct breakup process can be described as a 'quasi-sequential' process. Therefore, both resonant and non-resonant reactions are written [Sri88]

$$^{16}\mathrm{O} + {}^{208}\mathrm{Pb} \longrightarrow {}^{16}\mathrm{O}^* + {}^{208}\mathrm{Pb} \longrightarrow {}^{12}\mathrm{C} + \alpha + {}^{208}\mathrm{Pb}\,. \qquad (2.21)$$

Scattering can be described by the classical Rutherford law or by a DWBA (Distorted-Wave Born Approximation) calculation. In both cases, the excitation process is calculated in first-order perturbation theory. In the first section, the semiclassical approach will be used to extract the virtual photons from the Coulomb field and estimate the photonuclear cross section, and consequently the radiative-capture cross section making use of the detailed-balance theorem. The second section will explain how to take into account the nuclear interaction effects.

2.2.2 Semiclassical model

The semiclassical model of the Coulomb dissociation describes the ^{16}O and ^{208}Pb nuclei as classical objects moving on a hyperbolic trajectory with respect to each other. The excitation probablities of a nucleus are calculated with the first-order perturbation theory in order to extract the number of virtual photons that can participate to the excitation process. Such an assumption is valid if three conditions are fulfilled [Kie99]:

1– The de Broglie wavelength of the system $\hbar/mV$, where m is the reduced mass, must be small enough when compared to the distance of closest approach on the hyperbolic trajectory, given by $2Z_O Z_{Pb}\, e^2/E_O$. This leads to the condition

$$\eta = \frac{Z_O Z_{Pb}\, e^2}{\hbar V} \gg \frac{1}{4}\,, \qquad (2.22)$$

where η is the Sommerfeld parameter, and Z_O and Z_{Pb} are the charge numbers of ^{16}O and ^{208}Pb, respectively. In the case $E_O = 80$ MeV/u ($V \simeq 0.390\ c$) one has $\eta \simeq 12.3$.

2– The excitation process must not appreciably modify the trajectory, i.e. $E^* \ll E_O$, where E^* is the excitation energy (equal to E_γ, the

energy of the virtual photon). In practice, E^* is a few MeV while E_O is of the order of GeV.

3– The nuclei must not touch or interpenetrate in order to avoid nuclear-interaction effects. Thus, for a relative energy higher than the Coulomb-potential barrier, the distance of approach a must be greater than the sum of the nuclear radii, with $a = D + \sqrt{D^2 + b^2}$, where b is the impact parameter and $D = Z_O Z_{Pb} e^2/mV^2$ is half the distance of closest approach when $b = 0$. Therefore, $b > (R_O + R_{Pb})\sqrt{1 - 2D/(R_O + R_{Pb})}$; for high energies, this can be approximated to $b > R_O + R_{Pb} - D$.

After scattering, the projectiles are distributed on a cone, the opening of which depends on the impact parameter. The differential cross section is given by the Rutherford law [Val89a]:

$$\frac{d\sigma_R}{d\Omega} = \frac{D^2}{4} \frac{1}{\sin^4 \frac{\Theta}{2}} , \tag{2.23}$$

where $\Theta = 2 \arctan(D/b)$ is the scattering angle.

The impact parameter is thus strictly limited by the interpenetration and adiabaticity conditions: $R_O + R_{Pb} - D \lesssim b \lesssim 2\gamma V\hbar/E^*$, which corresponds, for $E^* = 9.84$ MeV and $E_O = 80$ MeV/u to a scattering angular range of

$$3.0^\circ \lesssim \Theta \lesssim 4.9^\circ . \tag{2.24}$$

The lower limit decreases at lower energy and the higher limit increases with a smaller reduced radius (this was here chosen 1.3 fm; it will be shown in section 2.2.3 that this is actually smaller for this reaction).

Transition probabilities

Since the trajectory is not appreciably modified by the excitation process (condition 2), the excitation cross section of ^{16}O from an initial state $|\psi_O\rangle$ of eigen energy E_0 ($E_0 = 0$ for ground state) to a final state $|\psi_{O^*}\rangle$ of eigen energy $E_0 + E^*$ can be expressed in the double-differential form

$$\frac{d^2\sigma^{exc}}{d\Omega dE}(E^*, \Theta) = \frac{d\sigma_R}{d\Omega}(\Theta) \, \frac{dP^{exc}}{dE}(E^*, \Theta) , \tag{2.25}$$

where dP^{exc}/dE is the probability per unit energy to find the system in the state $|\psi_{O^*}\rangle$ for a given angle Θ (or equivalently an impact parameter b) and defined as

$$\frac{dP^{exc}}{dE} = |a_1|^2 \,, \tag{2.26}$$

with the system described by the wave function

$$|\psi\rangle = a_0(t)\, e^{-i\frac{E_0}{\hbar}t}\, |\psi_O\rangle + a_1(t)\, e^{-i\frac{E^*}{\hbar}t}\, |\psi_{O^*}\rangle \,, \tag{2.27}$$

and with $a_1 \ll a_0$, which allows to apply first-order perturbation theory. Let $\mathcal{H} = \mathcal{H}^{(0)} + \mathcal{H}^{(1)}$ be the total Hamiltonian of the perturbed system, where $\mathcal{H}^{(0)}$ is the non-perturbative Hamiltonian and $\mathcal{H}^{(1)}$ is the first-order transition Hamiltonian. The time-dependent Schrödinger equation

$$\left(\mathcal{H}^{(0)} + \mathcal{H}^{(1)}\right) |\psi\rangle = i\hbar \frac{d}{dt} |\psi\rangle \tag{2.28}$$

is solved by inserting eq. 2.27 and multiplying by $\langle\psi_{O^*}|$. One finds

$$a_1 = \frac{1}{i\hbar} \int_{-\infty}^{+\infty} \langle\psi_{O^*}|\, \mathcal{H}^{(1)}\, |\psi_O\rangle\, e^{i\omega t} dt \,, \tag{2.29}$$

where $\omega = E^*/\hbar$.

A second-order process would have to take into account multiple-photon excitation but this has been shown to be negligible [Tat96] in most transitions.

Each Hamiltonian and transition amplitude is now split into electric and magnetic components. If the relative velocity is small compared to the speed of light and if a point-charge distribution is assumed for the constituents of the projectile and target clusters, the total-electric interaction Hamiltonian is written as a local scalar field coupling [Boh69, Ald75] integrated over the nuclear volumes:

$$\mathcal{H}_E(t) = \int_{\tau_{Pb}} \int_{\tau_O} \frac{\rho_{Pb}(\vec{r}_2)\; \rho_O(\vec{r}_1)}{\left|\vec{R}(t) + \vec{r}_1 - \vec{r}_2\right|} \, d\tau_O \, d\tau_{Pb} \,, \tag{2.30}$$

where $\vec{r}_1(r_1, \theta_1, \phi_1)$ defines a position in the ^{16}O centre-of-mass frame and $\vec{r}_2(r_2, \theta_2, \phi_2)$, a position in the ^{208}Pb centre-of-mass frame. τ_O and

τ_{Pb} refer to the ^{16}O and ^{208}Pb nuclear volumes, respectively. $\vec{R}(R,\theta,\phi,t)$ is the vector between the centres of mass of lead and oxygen. $\rho_O(\vec{r}_1)$ is the charge density in the projectile and $\rho_{Pb}(\vec{r}_2)$ is the charge density in the target, each of them being described by a point-charge nucleon distribution, given by $\rho(\vec{r}) = \sum_{k=1}^{A} e_k\ \delta(\vec{r} - \vec{r}_k)$, where δ is the Dirac delta-function and e_k and $\vec{r}_k$ are the charge and position of the k^{th} nucleon (see fig. 2.4).

Assuming that the nuclei do not interpenetrate (which implies the condition $r_1 + r_2 < R$), the denominator in eq. 2.30 is expanded into multipole components. The monopole-monopole ($\vec{R}$) and multipole-monopole ($\vec{R} - \vec{r}_2$) terms do not give rise to excitation in the projectile but only influence the relative motion since they do not depend

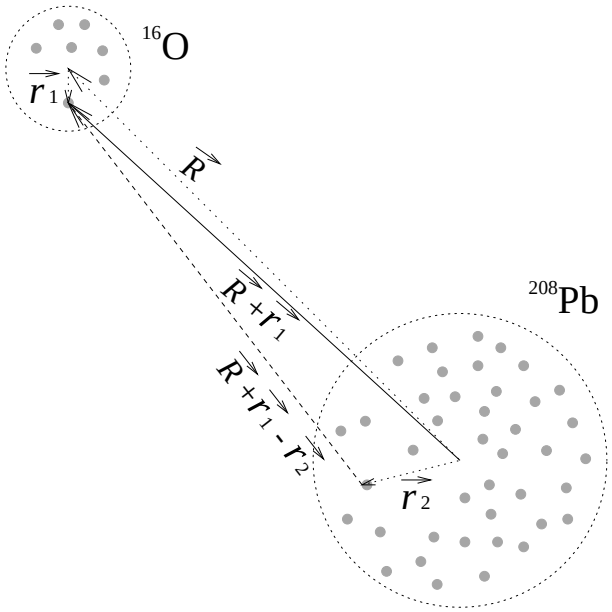

Figure 2.4: *The electric interaction can be described as a scalar field coupling between each point-charge constituent of the target and of the projectile ($\vec{R} + \vec{r}_1 - \vec{r}_2$). The monopole-multipole interaction in ^{16}O is the coupling between the monopole term of the target distribution and the multipole terms of the projectile ($\vec{R} + \vec{r}_1$).*

on the projectile nuclear internal degrees of freedom. Therefore, they are responsible for the non-perturbative electric Hamiltonian $\mathcal{H}_E^{(0)}$ (elastic scattering). Moreover, consistently with the first-order perturbation theory, the high-order multipole-multipole terms ($\vec{R}+\vec{r}_1-\vec{r}_2$) can be neglected [Ald75]. Therefore, only the monopole-multipole ($\vec{R}+\vec{r}_1$) terms are considered [Boh69] and the first-order electric-transition Hamiltonian can be expanded into spherical-tensor components as follows:

$$\mathcal{H}_E^{(1)}(t) = 4\pi Z_{Pb}\, e \sum_{l=1}^{\infty} \sum_{m=-l}^{+l} \frac{1}{2l+1} \frac{\mathcal{Y}_{lm}(\hat{r}(t))}{R(t)^{l+1}} \int_{\tau_O} \rho(\vec{r}_1)\; r_1^l\; \mathcal{Y}^*_{lm}(\hat{r}_1)\; d\tau_O, \quad (2.31)$$

where $\mathcal{Y}_{lm}$ are the normalised spherical harmonics.

Inserting the electric multipole moment defined by eq. 2.12 with eq. 2.31 into eq. 2.29 and making use of the property $\mathcal{Y}^*_{lm} = (-1)^m\, \mathcal{Y}_{l\,-m}$, the electric transition amplitude can be expressed in the form

$$a_E^{exc} = \frac{4\pi Z_{Pb}\, e}{i\hbar} \sum_{l>0\, m} \frac{(-1)^m}{2l+1} \langle \psi_{O^*} |\, \mathcal{M}_{El\,-m}\, | \psi_O \rangle\, \mathcal{S}_{Elm}(\omega)\,, \quad (2.32)$$

where the Coulomb-orbital integrals containing the dynamical information are defined as

$$\mathcal{S}_{Elm}(\omega) = \int_{-\infty}^{+\infty} \frac{e^{i\omega t}}{R(t)^{l+1}}\; \mathcal{Y}_{lm}(\hat{r}(t))\; dt\,. \quad (2.33)$$

The moment includes the structure information, i.e. position, velocity and spin of the nucleons and contains the isoscalar and isovector contributions.

Analogous to the electric interaction, the total magnetic-interaction Hamiltonian can be described by vector-field coupling [Ald56]:

$$\mathcal{H}_M(t) = -\frac{1}{c^2} \int_{\tau_{Pb}} \int_{\tau_O} \frac{\vec{j}_O(\vec{r}_1) \cdot \vec{j}_{Pb}(\vec{r}_2)}{\left| \vec{R}(t) + \vec{r}_1 - \vec{r}_2 \right|}\, d\tau_O\, d\tau_{Pb}\,, \quad (2.34)$$

where $\vec{j}_O$ and $\vec{j}_{Pb}$ are the projectile and target current densities, respectively. Expanding the monopole-multipole elements, the first-order magnetic-transition Hamiltonian is written [Ald56]

$$\mathcal{H}_M^{(1)}(t) = -\frac{4\pi Z_{Pb}\, e}{c^2} \sum_{l=1}^{\infty} \sum_{m=-l}^{+l} \frac{1}{l(2l+1)(l+1)} \times \frac{\mathcal{Y}_{lm}(\hat{r}(t))}{R(t)^{l+1}} \int_{\tau_O} \vec{\mathcal{L}} \cdot \vec{V}\ \vec{\mathcal{L}}_1 \cdot \vec{\jmath}_O(\vec{r}_1)\ r_1^l\ \mathcal{Y}^*_{lm}(\hat{r}_1)\ d\tau_O\,, \quad (2.35)$$

where $\vec{\mathcal{L}} = -i(-\vec{R}) \times \vec{\nabla}$ is the angular-momentum operator acting on the target and $\vec{\mathcal{L}}_1 = -i\,\vec{r}_1 \times \vec{\nabla}$ is that acting on the projectile constituents. Inserting the magnetic multipole moment as defined in eq. 2.13, the magnetic transition amplitude has a form analogous to the electric one:

$$a_M^{exc} = \frac{4\pi Z_{Pb}\, e}{i\hbar} \sum_{l>0\, m} \frac{(-1)^m}{2l+1} \langle \psi_{O^*} |\, \mathcal{M}_{Ml\,-m}\, |\psi_O\rangle\, \mathcal{S}_{Mlm}(\omega)\,, \quad (2.36)$$

with

$$\mathcal{S}_{Mlm}(\omega) = \frac{i}{c} \int_{-\infty}^{+\infty} \vec{\mathcal{L}} \cdot \vec{V}\ \frac{1}{l}\ \frac{e^{i\omega t}}{R(t)^{l+1}}\ \mathcal{Y}_{lm}(\hat{r}(t))\ \ dt\,. \quad (2.37)$$

Therefore, the transition amplitude can be split such that $a_1 = \sum_{lm} a^{exc}_{Elm} + a^{exc}_{Mlm}$. Thus, the transition probabilities can be expressed according to the various l channels:

$$\frac{dP^{exc}_{\Pi l}}{dE} = \sum_m |a^{exc}_{\Pi lm}|^2\ . \quad (2.38)$$

Note that the ^{16}O ground state is spinless thus the spin of the final state equals l. In a more general case the probability is summed over all initial and final magnetic substates rather than over subchannels m, and averaged over the number of initial substates.

The differential cross section for a given multipolarity can now be written

$$\frac{d^2\sigma^{exc}_{\Pi l}}{d\Omega dE}(E^*, \Theta) = \frac{d\sigma_R}{d\Omega}(\Theta)\ \frac{dP^{exc}_{\Pi l}}{dE}(E^*, \Theta)\,. \quad (2.39)$$

Relativistic treatment

For relativistic collisions ($v \simeq c$), the straight-line approximation, which consists in neglecting the deviation of the projectile (see fig. 2.5), can be applied. The treatment is parallel to that of the non-relativistic case and has been described in detail by Winther and Alder [Win78] and is summarised below.

In the coordinate system centred on ^{208}Pb nucleus, and having $\vec{R} + \vec{r}_1 = \vec{x} + \vec{y} + \vec{z}$, the Lienard-Wiechert relativistic Coulomb field produced by ^{208}Pb is given by [Jac75]

$$\varphi(\vec{R} + \vec{r}_1, t) = \frac{\gamma Z_{Pb}\, e}{\sqrt{(b-x)^2 + y^2 + \gamma^2 (z - Vt)^2}}\,, \tag{2.40}$$

and the vector potential is

$$\vec{A}(\vec{R} + \vec{r}_1, t) = \frac{\vec{V}}{c}\, \varphi(\vec{R} + \vec{r}_1, t)\,. \tag{2.41}$$

The Fourier transform of φ gives the frequency spectrum at the position $\vec{R} + \vec{r}_1$:

$$\varphi(\vec{R} + \vec{r}_1, \omega) = \frac{2 Z_{Pb}\, e}{V}\, e^{i \frac{\omega}{V} z}\, K_0 \left(\frac{\omega}{\gamma V} \sqrt{(x-b)^2 + y^2} \right)\,, \tag{2.42}$$

where K_0 is the modified Bessel function. This can be written in spherical tensor elements as follows:

$$\varphi(\vec{R} + \vec{r}_1, \omega) = \sum_{lm} W_{lm}(\vec{R} + \vec{r}_1, \omega)\; \mathcal{Y}^*_{lm}(\hat{R} + \hat{r}_1)\,, \tag{2.43}$$

where

$$W_{lm}(\vec{R} + \vec{r}_1, \omega) = \int_{4\pi} \varphi(\vec{R} + \vec{r}_1, \omega)\; \mathcal{Y}_{lm}(\hat{R} + \hat{r}_1)\; d\Omega\,. \tag{2.44}$$

This quantity can be analytically calculated and permits to find the electric and magnetic Hamiltonians from eqs. 2.30 and 2.34. Once inserted in eq. 2.29, the transition amplitudes can be written [Win78, Ber88]

$$a^{exc}_{\Pi lm} = -i\; (-1)^m \frac{Z_{Pb}\, e}{\hbar \gamma V} \sqrt{2l+1}\; \left(\frac{\omega}{c}\right)^l \times \\ G_{\Pi lm}\left(\frac{c}{V}\right)\; K_m\left(\frac{\omega b}{\gamma V}\right)\; \langle \psi_{O^*} |\, \mathcal{M}_{\Pi l\, -m}\, | \psi_O \rangle\;, \tag{2.45}$$

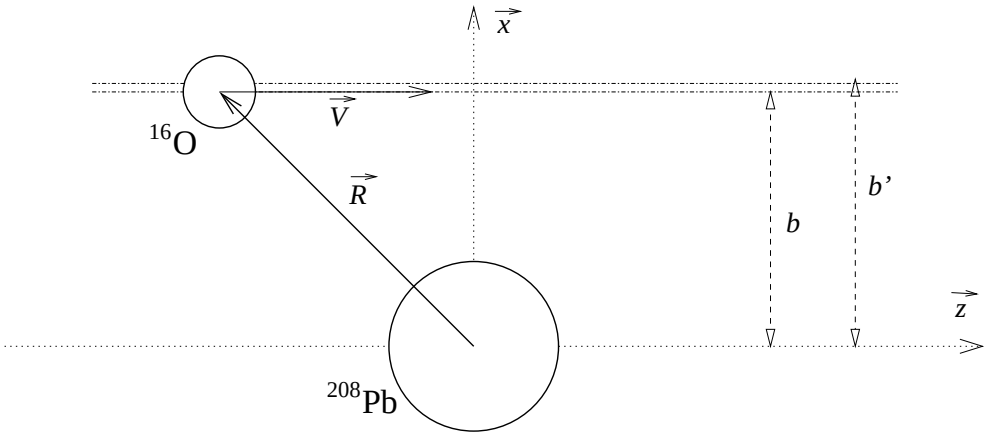

Figure 2.5: *For relativistic energies, the straight-line approximation neglects the projectile trajectory deflection when passing by the target. For intermediate energies, this approximation must take into account a field overestimation by replacing the impact parameter b by a corrected larger value b′.*

where $G_{\Pi lm}$ is a Gegenbauer integral (or Winther-Alder relativistic function, given in [Win78]) and K_m is a modified Bessel function. For intermediate energies, the projectile slightly deviates from the straight-line trajectory description and is on the average further away from the target. The field overestimation is then compensated by replacing the impact parameter by the corrected value $b' = b + \pi D/2\gamma$.

Excitation probabilities

The excitation differential cross section is given in eq. 2.39, by inserting eq. 2.45 into eq. 2.38:

$$\frac{dP^{exc}_{\Pi l}}{dE} = \left(\frac{Z_{Pb}\, e}{\hbar\gamma V}\right)^2 (2l+1)\left(\frac{\omega}{c}\right)^{2l} \times \left|\sum_m (-1)^m\, G_{\Pi lm}\left(\frac{c}{V}\right) K_m(\chi)\, \langle\psi_{O^*}|\, \mathcal{M}_{\Pi l\, -m}\, |\psi_O\rangle\right|^2 , \quad (2.46)$$

where $\chi = \omega b'/\gamma V$.

It is now practical to introduce the reduced transition probability, which contains all nuclear information, defined for a spinless ground

state as

$$B^{exc}_{\Pi l} = \sum_m \left| \langle \psi_{O^*} | \, \mathcal{M}_{\Pi l m} \, | \psi_O \rangle \right|^2 . \tag{2.47}$$

This value is strongly model-dependent and, in practice, this is the unknown that must be measured experimentally. Once $B^{exc}_{\Pi l}$ has been inserted in eq. 2.46, the final expression of the transition probabilities is written:

$$\frac{dP^{exc}_{\Pi l}}{dE}(E^*, \Theta) = \left(\frac{Z_{Pb}\, e}{\hbar \gamma V} \right)^2 (2l+1) \left(\frac{\omega}{c} \right)^{2l} B^{exc}_{\Pi l}(E^*) \times \sum_m \left| G_{\Pi l m}\left(\frac{c}{V} \right) K_m(\chi) \right|^2 . \tag{2.48}$$

The explicit results of this expression are detailed in appendix A.1 for each relevant multipolarity.

Detailed-balance theorem and photonuclear cross section

The ^{208}Pb(^{16}O,^{16}O*)^{208}Pb cross section has been evaluated with respect to the multipolarity, it is now necessary to express the cross section for the interaction of the photon with the projectile.

The absorption probability of a photon by a nucleus can be established in a symmetric way as the emission described in section 2.1.3, focusing at incoming waves instead of outgoing ones. The photonuclear cross section is then given by [Bla79]

$$\sigma^{\gamma}_{\Pi l} = \frac{8\pi^3 (l+1)}{l(2l+1)!!^2} \left(\frac{E_\gamma}{\hbar c} \right)^{2l-1} B^{exc}_{\Pi l}(E_\gamma) . \tag{2.49}$$

Independently, this can be expressed very generally as follows:

$$\sigma^{\gamma}_{\Pi l}(E_\gamma) = \pi \lambda\!\!\!^{-2}_{\gamma} \frac{2l+1}{2} \left| \langle \psi_{O^*} | \, \mathcal{H}_2 \, | \psi_{O\gamma} \rangle \, \langle \psi_{C\alpha} | \, \mathcal{H}_1 \, | \psi_{O^*} \rangle \right|^2 , \tag{2.50}$$

where $\lambda\!\!\!^{-}_{\gamma}$ is the photon reduced wavelength and 1/2 is a statistical factor due to the photon's spin. The radiative-capture cross section described in eq. 2.4 can be written in the form [Rol88]

$$\sigma^{cap}_{\Pi l} = \pi \lambda\!\!\!^{-2}_{C\alpha} (2l+1) \left| \langle \psi_{O^*} | \, \mathcal{H}_1 \, | \psi_{C\alpha} \rangle \, \langle \psi_{O\gamma} | \, \mathcal{H}_2 \, | \psi_{O^*} \rangle \right|^2 , \tag{2.51}$$

where $\mathcal{H}_1$ and $\mathcal{H}_2$ are the capture and dissociation Hamiltonians, respectively.

From eqs. 2.50 and 2.51, the time-reversal invariance principle permits to write the photonuclear cross section $\sigma^{\gamma}_{\Pi l}$ with respect to the radiative-capture cross section $\sigma^{cap}_{\Pi l}$ in the form of the detailed-balance theorem:

$$\sigma^{\gamma}_{\Pi l} = \frac{1}{2}\left(\frac{k_{C\alpha}}{k_{\gamma}}\right)^2 \sigma^{cap}_{\Pi l}\,, \tag{2.52}$$

where $k_{C\alpha} = \sqrt{2\mu\varepsilon}/\hbar$ and k_{γ} are the wave numbers of the ^{12}C+α system and of the photon, respectively. For a general reaction a(b,γ)c, this expression is multiplied by a statistical factor $(2I_a+1)(2I_b+1)/(2I_c+1)$, where I_a, I_b and I_c are the spins of the particles.

Eqs. 2.16 and 2.49 are introduced in the latter in order to write the following relationship [Sri88]:

$$B^{exc}_{\Pi l}(E_{\gamma}) = \frac{\mu\varepsilon}{\pi^2\hbar^3}(2l+1)B^{cap}_{\Pi l}(\varepsilon)\,, \tag{2.53}$$

which gives the possibility to calculate the capture cross section from the Coulomb-breakup measurements for reactions involving spin-0 particles.

Finally, for a resonant state of energy E^*, the integration of this value over the total width Γ of the resonance gives the reduced transition probability of excitation for this level:

$$B^{E^*}_{\Pi l} = (2l+1)\frac{l(2l+1)!!^2}{8\pi(l+1)}\left(\frac{\hbar c}{E^*}\right)^{2l+1}\Gamma_{\gamma}\,. \tag{2.54}$$

Virtual-photon spectrum

The number of virtual photons present in the Coulomb field is, in principle, given by the Fourier transform of the time-dependent electromagnetic Hamiltonians [Jac75, Gol84], but it is easier to calculate it as follows. The differential excitation cross section can be written [Ber85]

$$\frac{d\sigma^{exc}_{\Pi l}}{d\Omega}(E^*,\Theta) = \frac{dN_{\Pi l}}{d\Omega}(E_{\gamma},\Theta)\,\sigma^{\gamma}_{\Pi l}(E_{\gamma})\,\frac{1}{E_{\gamma}}\,. \tag{2.55}$$

Introducing eqs. 2.25, 2.48 and 2.49, one can write

$$\frac{dN_{\Pi l}}{d\Omega}(E_{\gamma},\Theta) = \frac{d\sigma_R}{d\Omega}\frac{Z^2_{Pb}\,e^2}{b'^2\hbar c}\frac{l(2l+1)!!^2}{8\pi^3(l+1)}\chi^2\sum_m\left|G_{\Pi lm}\left(\frac{c}{V}\right)K_m(\chi)\right|^2. \tag{2.56}$$

The results of this formula are given in appendix A.2 for each relevant multipolarity. The number of photons is plotted for each multipolarity as a function of the projectile velocity V and of the photon energy E_γ in fig. 2.6. This shows that the Coulomb excitation highly favours the quadrupole contribution [Sho92], by a factor of about 50 compared to that of the dipole at 80 MeV/u.

Angular correlation of the fragments

The previous calculation permits to find the double-differential cross section for a given multipolarity, scattering angle, and excitation energy. An angular correlation study requires to include the expansion of the magnetic substates by modifying the expression of the cross section as

$$\frac{d^3\sigma^{exc}_{\Pi l}}{dE\, d\Omega\, d\Omega_{cm}}(E,\Theta) = \frac{d\sigma_R}{d\Omega}\,\frac{d^2P^{exc}_{\Pi l}}{dE\, d\Omega_{cm}}\,, \tag{2.57}$$

where Ω_{cm} is the solid angle where one of the fragments is emitted (see fig. 2.7). The angles of the other fragment are given by $\theta_{\alpha cm} = \pi - \theta_{Ccm}$, $\phi_{\alpha cm} \equiv \pi + \phi_{Ccm}\,[2\pi]$. For spinless particles, the dissociation probability can be expressed as [Bau89]

$$\frac{d^2P^{dis}_{\Pi l}}{dE\, d\Omega_{cm}} = \left|\sum_m a^{exc}_{\Pi l m}\, \mathcal{Y}_{lm}(\theta_{cm},\phi_{cm})\right|^2 . \tag{2.58}$$

The actual fragment angular correlation has to take account of the interferences between the various multipolarities. This is described by a coherent sum of the probabilities with a mixing angle. It was shown [Red87, Bau89, Tat95, Tat96] that, despite a low dipole strength, an important interference effect appears in the continuum, which can be used to measure precisely the relative multipole contributions.

2.2.3 Nuclear effects and the optical model

Description of the model

It was already mentioned that the semiclassical description breaks down when the ^{16}O and ^{208}Pb nuclei interpenetrate. In practice, the scattering angle range that allows the use of the semiclassical approximation

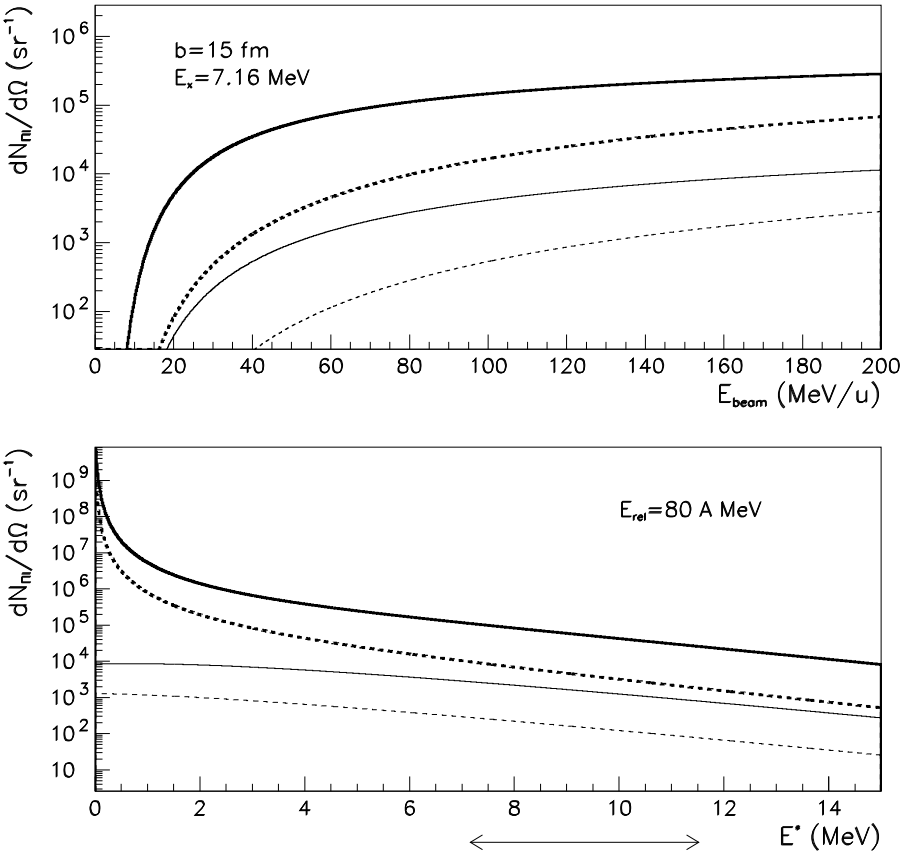

Figure 2.6: *The top figure displays 7.16 MeV-photon intensities per unit solid angle at 15 fm impact parameter for E2, M2, E1 and M1 multipolarities (from top to bottom, respectively) as functions of the relative energy between the projectile and target nuclei. The bottom figure is the virtual-photon spectrum for each of these multipolarities at 80 MeV/u relative energy. The region of interest is shown by the double arrow, between 7.16 and 11.52 MeV.*

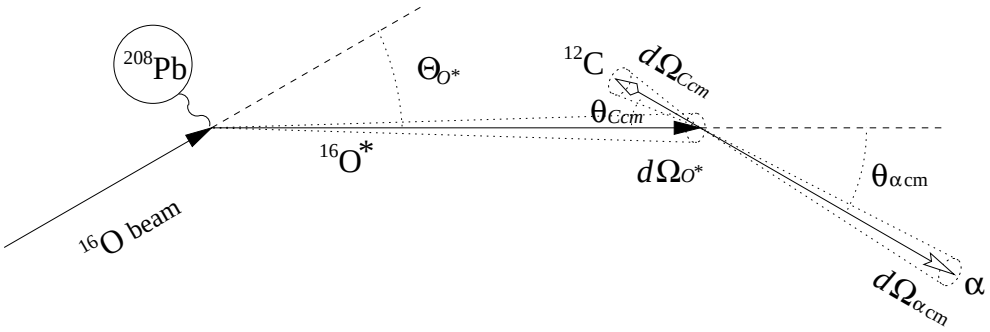

Figure 2.7: *Definition of the angles used for the triple-differential cross section. For clarity, the nuclei are shown in the plane $\phi \equiv 0\ [\pi]$.*

is narrow (a few degrees) [Ber85]. Therefore, it is necessary to use a quantum-mechanical approach where the system is described by a wave function in a Coulomb plus nuclear potential. In the optical model, the Schrödinger equation is solved by expanding the wave function in partial waves. The Hamiltonian has a spherical average potential, which includes the Coulomb field as well as a nuclear field, the latter being composed of a real part and an imaginary part. This method has been shown to describe elastic scattering very accurately.

Excited nuclear systems are known to be well represented by a collective model [Tam65] that describes the excitation process by inducing a collective surface vibration of an incompressible (at low excitation energy) liquid drop, or a rotation. The vibration or the rotation is time-averaged so that the nucleus is described by a deformed potential. In spite of certain ambiguities, the deformed optical-potential model is known to provide a good description of the phenomenological inelastic scattering process [Jac70, Sat83].

The surface of the spherical drop satisfies the equations of hydrodynamics, the solution of which gives the sum of the waves in the form

$$R(\theta, \phi, t) = R_0 \left(1 + \sum_{l=2}^{+\infty} \sum_{m=-l}^{+l} \alpha_{lm}\ \mathcal{Y}^*_{lm}(\theta, \phi) \right) , \tag{2.59}$$

where $R_0 = R_{Pb} + R_O$ is the radius of the static potential, $\mathcal{Y}_{lm}$ is a spherical harmonic and α_{lm} is the dynamical amplitude operator of the corresponding phonon characterising the displacement of the drop surface for the given multipolarity. Note that the sum begins with $l = 2$

because a monopole vibration would correspond to a density oscillation (which is possible only at high excitation energies because of the large nuclear incompressibility), while a dipole vibration is unphysical since this would correspond to a spurious centre-of-mass motion.

The ^{16}O and ^{208}Pb nuclei interact via a complex Coulomb-nuclear potential $\mathcal{U} = V + W + iW'$, where V is the mean Coulomb potential and W and W' are the real and imaginary parts of the mean nuclear potential. The nucleon density is written in the form

$$\rho(r,\theta,\phi) = \frac{\rho_0}{1 + e^{\frac{r - R(\theta,\phi)}{a}}}\,, \tag{2.60}$$

where R is the nuclear radius given by eq. 2.59, a is the diffuseness and ρ_0 is a normalisation factor. Therefore, the Coulomb potential is given by

$$V(r,\theta,\phi) = \frac{1}{r}\int_\tau \rho(r',\theta,\phi)\, e^2\, d\tau\,, \tag{2.61}$$

where τ is the nuclear volume. The nuclear potential is assumed to have a Woods-Saxon form:

$$W(r,\theta,\phi) = -\frac{W_0}{1 + e^{\frac{r - R_W(\theta,\phi)}{a_W}}}\,, \tag{2.62}$$

where R_W is the potential radius given by eq. 2.59, a_W is the diffuseness and W_0 is the well depth. These are experimentally determined by fitting the measured elastic scattering cross section to optical-model calculations with the given nuclear optical potential. W' has a similar form with parameters $R_{W'}$, $a_{W'}$ and W'_0. For a small deformation, each potential can be expanded in Taylor series near the static radius R_{0U} such that

$$U(r,R_U) = U(r,R_{0U}) + (R_U - R_{0U})\frac{dU(r,R_{0U})}{dR_U} + \ldots\,, \tag{2.63}$$

where U can be V, W or W'. The first term is the static (spherical) optical interaction potential that scatters particles elastically while the second is the first-order transition potential.

Inserting eq. 2.59 in the latter, the first-order transition potential from the ground state to the state $|l\rangle$ can then be written in the form

$$\langle l|\, U_l(r,R_U)\,|0\rangle = \frac{\beta_{lU} R_{0U}}{\sqrt{2l+1}}\frac{dU(r,R_{0U})}{dR_U}\,, \tag{2.64}$$

Table 2.1: *Parameters of the optical potential determined by Roussel-Chomaz et al. [Rou88] from fitting elastic scattering data of $^{208}Pb(^{16}O,^{16}O)^{208}Pb$at 94 MeV/u. Note that $R_{0W} = R_{0W'}$ and $a_W = a_{W'}$.*

W_0 (MeV)	R_{0W} (fm)	a_W (fm)	W_0' (MeV)	$R_{0W'}$ (fm)	$a_{W'}$ (fm)
80	9.053	0.718	51.6	9.053	0.718

where β_{lU} is the deformation parameter, i.e. the amplitude of the time-averaged global oscillation for the multipolarity l. If this equation actually generates one deformation parameter for each potential, in practice the deformation lengths are assumed to be equal [Sat83] so that $\beta_{lV}R_{0V} = \beta_{lW}R_{0W} = \beta_{lW'}R_{0W'}$. The complex Coulomb-nuclear transition potential from the ground state to the state $|l\rangle$ can thus be written

$$\langle l|\,\mathcal{U}_l(r, R_V, R_W, R_{W'})\,|0\rangle = \frac{\beta_l R_0}{\sqrt{2l+1}}\left(\frac{dV(r, R_{0V})}{dR_V} + \frac{dW(r, R_{0W})}{dR_W} + \frac{dW'(r, R_{0W'})}{dR_{W'}}\right). \quad (2.65)$$

The parameters of the optical potential have been determined from fitting elastic scattering data of ^{16}O on ^{208}Pb obtained at 94 MeV/u by Roussel-Chomaz et al. [Rou88]. These are listed in table 2.1. It can be reasonably assumed that the neutron and proton nuclear distributions are similar. Thus, the same radius R_0 is used for the Coulomb potential, and hence also the same β_l.

Angular distribution of $^{16}O^*$

Given the transition potential of eq. 2.65, the solution of the Schrödinger equation is obtained in the framework of coupled equations [Tam65]. The wave function $|\psi\rangle$ is expanded in $l+1$ partial waves, and the resulting system of equations is solved for the radial wave-function components of each of them.

This calculation is performed by sequential iterations with the ECIS code [Ray71]. If the calculation is stopped after one iteration, this would correspond to a DWBA calculation. For a given transition from a state $|I_i\rangle$ to a state $|I_f\rangle$, where I_i and I_f are the spins of these states, ECIS

computes every possible lm channel with the usual parity restrictions. This is performed for all entrance angular momenta from $L = 0$ to a 'sufficiently' large value. This leads to the exit channels $L'M'$ such that $\vec{L'} = \vec{L} - \vec{l}$, with $\vec{l} = \vec{I_f} - \vec{I_i}$ is the transferred angular momentum. The output file contains the scattering-matrix (or S-matrix) elements as well as the differential cross sections given for the corresponding scattering-angle range.

The total multipole moment for a vibrational phonon state $|l\rangle$ with vibrational deformation parameter β_l is given by [Sat83]

$$\sum_m \mathcal{M}_{\Pi lm} = \frac{\beta_l}{\sqrt{2l+1}} \int R_0 \frac{d\rho(r, R_O)}{dR_0}\, r^{l+2}\, dr\,. \tag{2.66}$$

The reduced transition probability $B^{E^*}_{\Pi l}$, from the ground state to an excited state of energy E^*, defined in eq. 2.47, can now be expressed making use of eq. 2.66 as a function of the deformation parameter as [Sat83]

$$B^{E^*}_{\Pi l} = \left| \frac{1}{4\pi}(l+2)\beta_l Z_O R_0 \left\langle r^{l-1} \right\rangle \right|^2 e^2\,. \tag{2.67}$$

The calculations were done for the 2^+ states at 9.84 and 11.52 MeV with the input files given in appendix B. The reduced transition probabilities $B^{E^*}_{E2}$ are computed from eq. 2.54 with the resonance widths tabulated in [Ajz86]. Consequently, the deformation parameters β_2 are calculated from eq. 2.67. The result of the DWBA calculation for the state at 11.52 MeV, with the transition potential and deformation parameter determined as described above, is plotted in fig. 2.8. The differential cross section displays a pattern that is sensitive to the interference between the Coulomb and nuclear amplitudes. The comparison with the semiclassical model calculations show that the latter is consistent with the Coulomb part of the DWBA calculation in terms of the integrated cross section. These agree with each other within 2%.

The 2^+ state at 9.84 MeV is known to be populated via a coupling with the 2^+ state at 6.92 MeV [Har76]. Therefore, coupled-channel calculations involving these states are necessary to calculate the differential cross section for the state at 9.84 MeV. This shows a typical offset when compared to the calculation with a one-step direct excitation from the ground state.

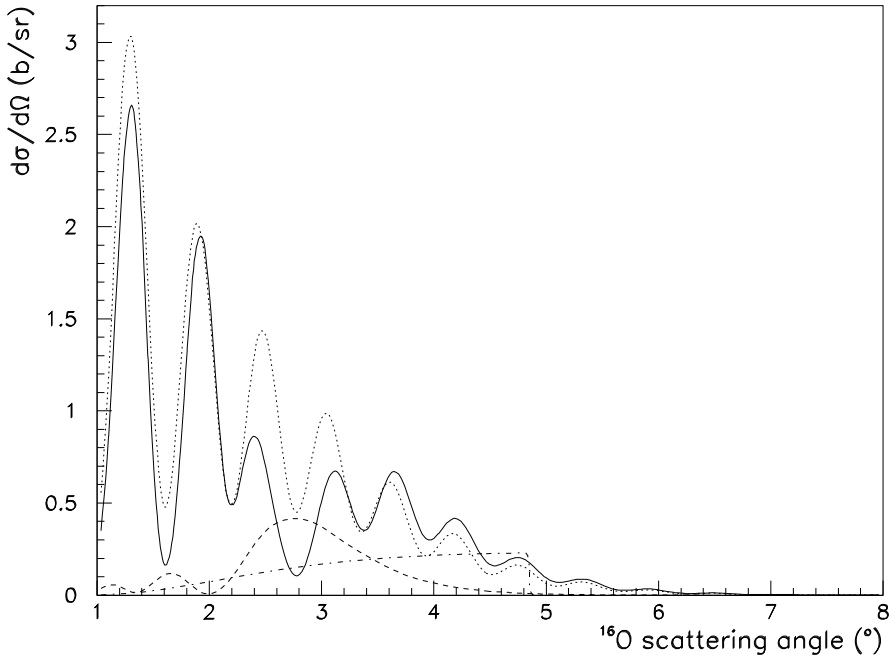

Figure 2.8: *DWBA calculation performed with ECIS [Ray71]. The figure displays for the scattering of an ^{16}O projectile from a ^{208}Pb target at 80 MeV/u the total nuclear-Coulomb (solid line) differential cross section in comparison with those of pure nuclear (dotted line) and pure Coulomb (dashed line) excitation of the 2^+ resonance at 11.52 MeV. A destructive interference between Coulomb and nuclear amplitudes is clearly visible in the angular range 2.4°–3.2°. For comparison, the dash-dotted line is the semiclassical calculation with a cut at the grazing angle. The integrated semiclassical cross section is the same as that of the Coulomb part of the optical model within 2%. Calculations for the same multipolarity at other energies show nearly an identical shape for the differential cross section.*

Both states show an important destructive interference of the nuclear and Coulomb interactions visible between 2° and 3°. This is precious information to test the validity of the model and the accuracy of the description of both contributions and of their relative strength.

The folded-potential model approach

In comparison with the deformed-potential model, which is of a phenomenological nature, the folded-potential model is a theoretically more descriptive approach. While in the former, the potential is determined by fitting elastic-scattering data, the folded potential is built by explicitly folding the nucleon-nucleon interaction over the target and projectile density distributions. The transition potential analogous to that given by eq. 2.64 is written in the form [Bee96]

$$\langle l|\, G_l(r)\, |0\rangle = \int g_l(r')\bar{v}_l(r,r')r'^2 dr'\,, \tag{2.68}$$

where g_l is the transition density and $\bar{v}_l$ is the 2^l component of the nucleon-nucleon interaction averaged over the ground-state density distribution. g_l is given, like for the deformed potential, by

$$g_l(r) = \frac{\beta_{lU} R_{0U}}{\sqrt{2l+1}} \frac{d\rho(r)}{dr}\,. \tag{2.69}$$

An ECIS calculation was performed with the folded potential for the 2^+ resonance at 11.52 MeV [Kie02]. The result is plotted in fig. 2.9 compared to the result of the deformed-potential model calculation presented in the previous section. The general shape is similar for both models, but the cross section from the folded-potential model is lower by roughly 50 to 80% compared to the one from the deformed-potential model. There is also a phase shift of the order of 0.2°, and the interference pattern is clearly identifiable.

Angular correlation of the fragments

The $^{16}O^*$ m-substate population directly determines the angular correlation of the fragments in their centre of mass. It has been shown [Bau89,

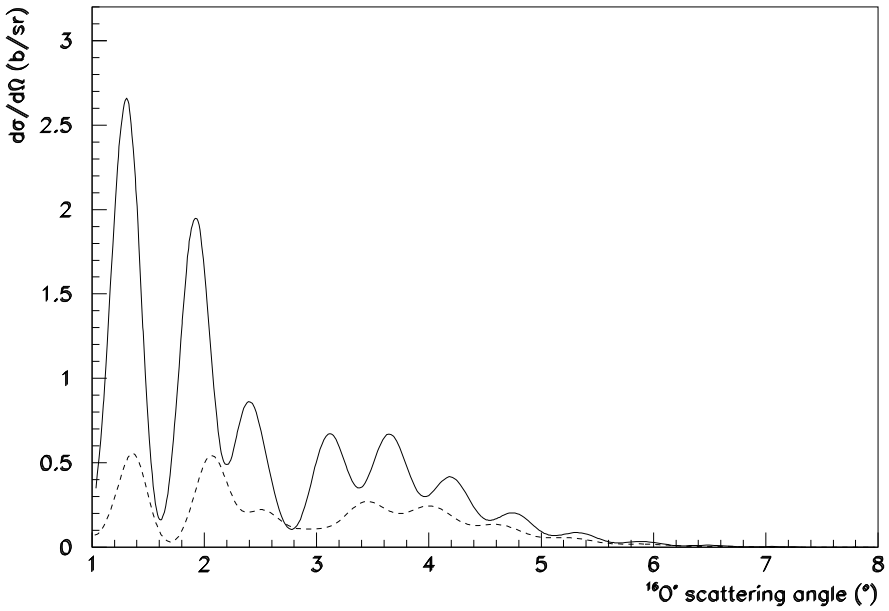

Figure 2.9: *Comparison of ECIS calculations with a deformed potential (solid line) and a folded potential (dashed line) for the 2^+ state at 11.52 MeV. They include both nuclear and Coulomb interfering contributions. They show an important cross-section discrepancy, and a small phase shift.*

Tat95, Tat96] that the angular correlation of the fragments is very sensitive to the interferences between the contributions of the various multipolarities involved in the excitation process. Therefore, this observable is a powerful tool to separate the contributions of the different multipoles from one another.

ECIS solves the Schrödinger equation for each m substate for the given transferred angular momentum l, and computes every scattering-matrix element S_{lm}. It is then straightforward to calculate the integrated m-substate population of ^{16}O and thus the fragment angular-correlation

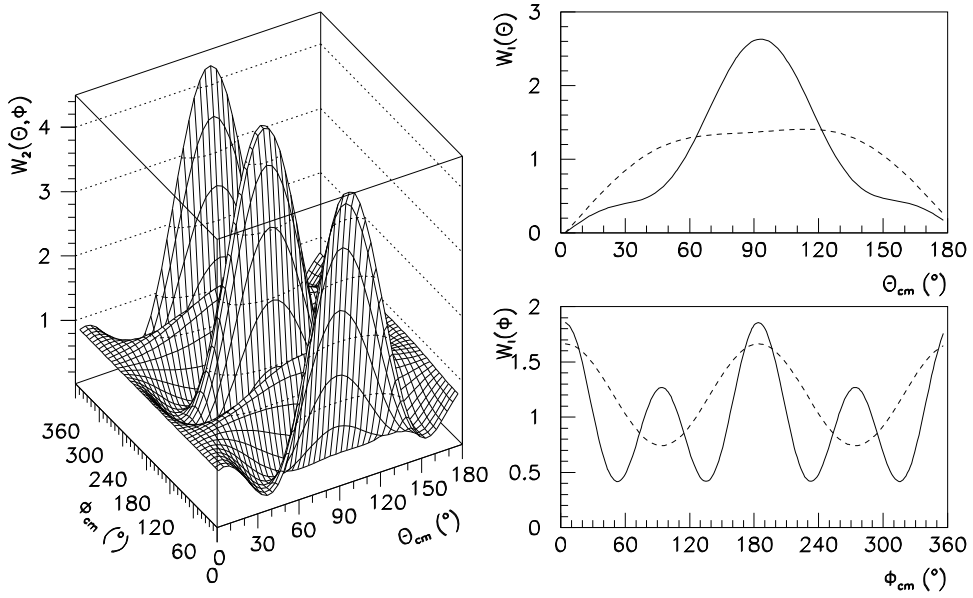

Figure 2.10: *Angular correlations of the fragments in the centre of mass, calculated from the S-matrix elements computed with ECIS. The left figure displays the two-dimensional correlation calculated for the* 2^+ *state at 11.52-MeV. The solid lines in the right figures are the normalised projections of the left one on the* θ_{cm} *and* ϕ_{cm} *axes. For comparison, the right figures also show the angular correlation for a* 1^- *state (dashed lines).*

function that can be written in the form [Sat83]

$$W_l(\theta,\phi) = \sum_m A_{lm}(\hat{k}_C, \hat{k}_\alpha) \left(\frac{4\pi}{2l+1}\right)^{\frac{1}{2}} \mathcal{Y}_{lm}(\theta,\phi)\,, \tag{2.70}$$

where the factor before the harmonics is a normalisation factor.

Fig. 2.10 shows the results of a calculation for the typical E2 angular correlation of the state at 11.52 MeV, and compares it to an E1 correlation. It appears clearly that the correlation of the fragments strongly characterises the multipolarity of the excitation.